arXiv:1611.04591v1 [cond-mat.quant-gas] 14 Nov 2016

Preparation of Low Entropy Correlated Many-body States via Conformal Cooling Quenches

Michael P. Zaletel,[1] Dan M. Stamper-Kurn,[2] and Norman Y. Yao[2]

[1]*Station Q, Microsoft Research, Santa Barbara, California 93106, USA*
[2]*Department of Physics, University of California Berkeley, Berkeley, CA 94720, U.S.A.*

We analyze a method for preparing low-entropy many-body states in isolated quantum optical systems of atoms, ions and molecules. Our approach is based upon shifting entropy between different regions of a system by spatially modulating the magnitude of the effective Hamiltonian. We conduct two case studies, on a topological spin chain and the spinful fermionic Hubbard model, focusing on the key question: can a "conformal cooling quench" remove sufficient entropy within experimentally accessible timescales? Finite temperature, time-dependent matrix product state calculations reveal that even moderately sized "bath" regions can remove enough energy and entropy density to expose coherent low temperature physics. The protocol is particularly natural in systems with long-range interactions such lattice-trapped polar molecules and Rydberg dressed atoms where the magnitude of the Hamiltonian scales directly with the density. To this end, we propose a simple implementation of conformal cooling quenches in a dilutely-filled optical lattice, where signatures of quantum magnetism can be observed.

Ultracold quantum gases have reached the extraordinary realm of sub-nanokelvin temperatures [1, 2], revealing, along the way, phenomena ranging from Bose-Einstein condensation and Cooper-paired superfluidity to Mott insulators and localization [3–7]. This scientific impact owes, in part, to a flexible array of cooling techniques that can effectively quench the kinetic energy of atomic systems; indeed, the laser cooling of atomic registers in optical tweezers has enabled the observation of few-particle quantum interference and entanglement [8, 9], while the evaporative cooling of Bose gases has realized temperatures nearly two orders of magnitude smaller than that required for condensation [10].

Nevertheless, these temperatures are still too high to emulate a number of more exotic- and delicate- quantum phases including antiferromagnetic spin liquids, fractional Chern insulators and high-temperature superconductivity [11–13]. The figure of merit for observing such physics is not the absolute temperature, but rather the dimensionless entropy density in units of k_B [14]. Reaching ultra-low entropy densities remains a major challenge for many-body quantum simulations despite the multitude of kinetic cooling techniques. This challenge is particularly acute for gases in deep optical lattice potentials, for which transport, and thus evaporative cooling, is slowed [15]. Moreover, in lattice systems representing models of quantum magnetism, the entropy resides primarily in spin, rather than motional, degrees of freedom [16]. Expelling such entropy through evaporative cooling requires the conversion of spin excitations to kinetic excitations, a process that is typically inefficient [17–19].

Two broad approaches have been proposed toward overcoming this challenge. The first is adiabatic preparation, where one initializes a low entropy state and changes the Hamiltonian gradually until the desired many-body state is reached [20, 21]. However, the final entropy density is bounded from below by the initial entropy density, and experimental constraints or phase transitions may preclude a suitable adiabat.

The second approach is to 'shift entropy elsewhere' [11, 22, 23], using the system's own degrees of freedom as a bath.

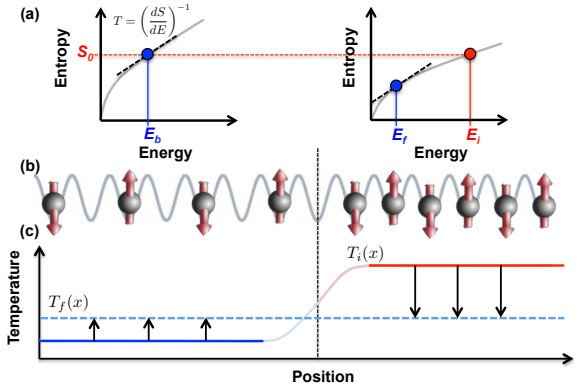

FIG. 1. a) If the Hamiltonian of a "bath" is related to that of the "system" by a constant rescaling, $H_B = \lambda H_S$, their entropy-energy-density curves satisfy $s_B(E) = s_S(E/\lambda)$. Thus preparing at state with constant entropy density establishes a temperature differential $T_B = \lambda T_S$, since $T = \frac{dE}{dS}$. b) Schematic representation of trapped polar molecules interacting through a long-range dipolar $1/R_{ij}^3$ potential. If the molecules in the left "bath" are diluted by a factor of r, then $H_B = (\frac{1}{r})^3 H_S$ [24]. c) In this case, a uniform Neél state has a temperature differential after reaching local equilibrium, and the resulting evolution will remove entropy from the right half of the chain as the system reaches global equilibrium.

Indeed, this approach helps to stabilize the Mott-insulating phase of the Bose-Hubbard model, where the low-density wings of the system serve as an entropy sink allowing for in-situ evaporative cooling.

In this work, we analyze a class of methods—termed 'conformal cooling quenches'—for shifting entropy by spatially modulating the magnitude of the Hamiltonian [25]. The intuition behind our approach is best illustrated as follows: Suppose that we take a system's Hamiltonian H and either suddenly or adiabatically reduce it by a factor $\lambda < 1$, taking $H \to \lambda H$. Since $k_B T$ has units of energy, the temperature T is accordingly reduced by $T \to \lambda T$. When applied to the entire system, this "cooling" is trivial, since it amounts to a change of units without reducing the entropy density. How-

ever, if the reduction by λ instead occurs for only a *portion* of the system, which we call the 'bath,' the change in temperature is physical, and establishes a temperature gradient; during equilibration, entropy will then flow out of the system and into the bath.

One virtue of the conformal cooling approach is that it can "cool" a system within a metastable state-space. For example, conforming cooling can be applied to a gas equilibrating at negative kinetic or spin temperature [26], bringing the system toward zero temperature from below. It can also be applied to gases equilibrating in high-energy manifolds of states, i.e. in excited bands of an optical lattice [27, 28]. Systems equilibrating at negative temperatures or in higher bands can exhibit strong frustration without complicated band engineering.We will begin by introducing the thermodynamics of our approach, focusing on two questions: 1) how much entropy can a cooling quench remove and 2) how long does it take? Next, we perform a numerical study of both a 1D toplogical spin-chain and the fermionic Hubbard model, demonstrating that realistic cooling quenches can remove enough entropy to reveal their low-temperature physics. Finally, we propose experimental implementations of our approach in systems with power-law interactions and the half-filled Fermi-Hubbard model.

General Strategy—We envision spatially demarcating the degrees of freedom into a "bath" (B) and "system" (S) which are placed "end-to-end," so that the coupling between their boundaries scales sub-extensively with their volume (Fig. 1b) [29]. We assume that the Hamiltonian H_B (bath) is identical to H_S (system), except that its magnitude is scaled by a factor $\lambda < 1$. The entropy (s) versus energy density (E) curves in the two regions are then related by $s_B(E) = s_S(E/\lambda)$ and their temperatures by $T_B(E) = \lambda T_S(E/\lambda)$ (Fig. 1a). In the following, we will consider two protocols, "quenched" and "adiabatic."

Quench Protocol—In the quench approach, the Hamiltonians are time-independent with $H_B = \lambda H_S$. At $t = 0$, we prepare a uniform initial state (e.g. a product state) and simply let it evolve. Equivalently, one can begin in thermal equilibrium with $H_B = H_S$, and then suddenly reduce H_B to $H_B = \lambda H_S$. The overall system is now in *local* equilibrium, with the local density matrices in B and S identical, and thus, $s_B = s_S$ and $T_B = \lambda T_S$. As the system evolves toward *global* equilibrium, entropy will follow the thermal gradient and flow from S to B. Thus, by probing region S, one can explore physics at an entropy density far lower than that of the initial state.

The final equilibrium temperature $T_{\rm f}^{(q)}$ is determined by energy conservation,

$$(V_S + \lambda V_B) E_S(T_{\rm i}) = V_S E_S(T_{\rm f}^{(q)}) + V_B \lambda E_S(T_{\rm f}^{(q)}/\lambda) \quad (1)$$

where V_S, V_B are the volumes of the system and bath and $T_{\rm i}$ is the initial temperature of the system. When $\lambda V_B \gg V_S$, we have $T_{\rm f}^{(q)} = \lambda T_{\rm i}$, but more generally one should choose λ so as to minimize $T_{\rm f}^{(q)}$ based on the precise form of $E_S(T)$.

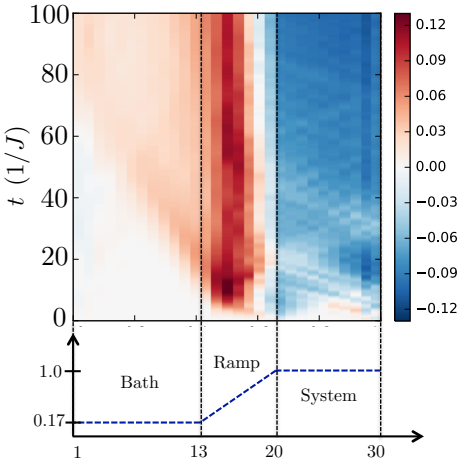

FIG. 2. 'Quench' cooling of a 30-site spin-1 Haldane chain. After initializing the state at $t = 0$ with uniform entropy density, the coupling constants λ_x are scaled according to the bottom panel, which should transport heat from the 'system' on the right to the 'bath' on the left. In the top panel, we plot the change in energy density $h_x(t) - h_x(0)$ as the chain evolves.

While we have assumed a sharp distinction between S and B for simplicity, one can let the spatial modulation $\lambda(\vec{x})$ vary smoothly, in which case Eq. (1) is replaced by an integral over the energy density.

Adiabatic Protocol—The cooling is more effective if the magnitude of $H_B = \Lambda(t) H_S$ is instead slowly reduced in time, with $\Lambda(t = 0) = 1$ and $\Lambda(t \to \infty) = \lambda$. In the isentropic limit, the final system temperature $T_{\rm f}^{(a)}$ is determined by

$$(V_B + V_S) s_S(T_{\rm i}) = V_B s_S(T_{\rm f}^{(a)}/\lambda) + V_S s_S(T_{\rm f}^{(a)}), \quad (2)$$

with $T_{\rm f}^{(a)} \leq T_{\rm f}^{(q)}$. When the bath and system are end-to-end, diffusive dynamics imply that the equilibration time, $t_{\rm eq}$, scales as $L_S^2/\Lambda(t)$ (q.v. Eq. (6)) where L_S is the linear extent of the system and adiabaticity requires $\partial_t \Lambda \ll 1/t_{\rm eq}$. For small Λ, the bath and system will eventually fall out of equilibrium and additional entropy will be produced, though the temperature will always be upper-bounded by $T_{\rm f}^{(q)}$.

To demonstrate that conformal cooling can shift significant entropy out of the system even for moderate bath sizes and short time-scales, we numerically investigate two distinct settings: the $S = 1$ Haldane topological anti-ferromagnet and the fermionic Hubbard model.

Conformal cooling in an $S = 1$ Haldane chain— Consider a one dimensional chain of $S = 1$ spins with Hamiltonian

$$H[\lambda_x] = \sum_x \lambda_x h_x = J \sum_x \lambda_x \left[\mathbf{S}_x \cdot \mathbf{S}_{x+1} + \frac{\gamma}{3} (\mathbf{S}_x \cdot \mathbf{S}_{x+1})^2 \right]. \quad (3)$$

At both the Heisenberg point $\gamma = 0$ and the AKLT point $\gamma = 1$, the spin-chain is a gapped topological paramagnet in the Haldane phase [30, 31]. The topology of the phase has

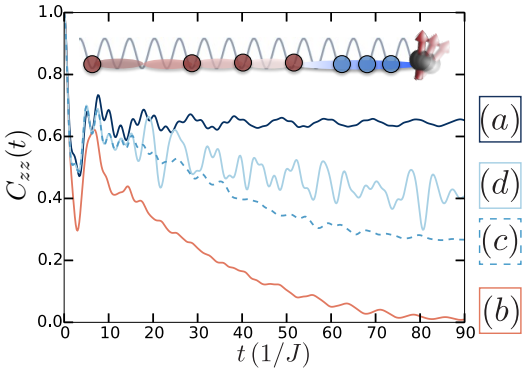

FIG. 3. Dynamical correlation $C_{zz}(t)$ measured after four initialization protocols: a) Optimal: $C_{zz}(t)$ for the ground state of an $L = 10$ chain; b) finite initial temperature $T_{\rm i} = 0.51J$, without a cooling quench. The edge coherence rapidly decays. c) finite $T_{\rm i} = 0.51J$, but starting the C_{zz} measurement after the cooling quench shown in Fig. 2. The coherence is improved by an order of magnitude. d) Same as (c), but eliminating the coupling between sites $i = 20$ and 21 after the quench, which cuts off the bath.

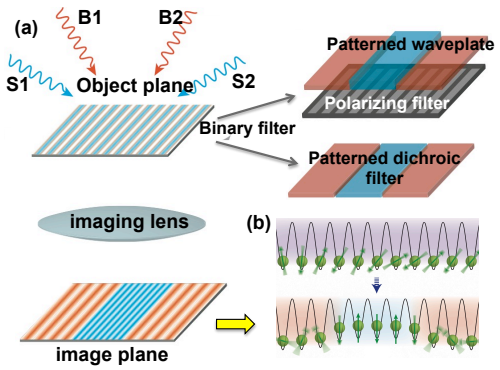

FIG. 4. a) Schematic of a "binary" optical potential based upon overlaying two distinct optical intensity patterns that are projected onto a single object plane. Binary filtering can be achieved using either a spatially patterned wave-plate followed by a polarizing filter or via a dichroic interference filter. b) The resultant binary potential modulates the depth of the optical lattice yielding a super-exchange Hamiltonian with smaller overall magnitude in the bath.

a striking signature in a finite-length chain, which has pair of localized spin-1/2 edge states. At temperatures below the bulk gap, $T < \Delta \sim J$, these localized edge states can coherently store quantum information for long times, providing a sharp experimental signature of the topological phase [32].

Calculating the thermodynamics using exact diagonalization reveals that a modest bath size of $V_B/V_S \approx$ 2-3 is sufficient to cool from the Neél product state $|\uparrow\downarrow\uparrow\downarrow\cdots\rangle$, which corresponds to an initial temperature $T_{\rm i} = 1.45\Delta$, to well below the gap, $T_{\rm f}^{(q)} \approx 0.7\Delta$ [33]. Since the spin chain is diffusive [34], the time-scale required for cooling is determined by Fourier's law. When $\lambda(x)$ varies smoothly compared to the lattice scale, the local thermal conductivity κ and specific heat c are determined by rescaling, $\kappa(T,x) = \lambda(x)\kappa_S(T(x)/\lambda(x))$ and $c(T,x) = c_S(T(x)/\lambda(x))$, where $\kappa_S(T)$ and $c_S(T)$ are defined with $\lambda = 1$. Applying this within a simple lumped element model predicts that temperature will decrease as [33],

$$T_S(t) \sim T_{\rm f}^{(q)} + \mathcal{K}\frac{L_S}{\sqrt{tD_B}}(T_{\rm i} - T_{\rm f}^{(q)}) \qquad (4)$$

where D_B is the thermal diffusivity of the bath, L_S is the linear extent of the system and $\mathcal{K}$ is an $\mathcal{O}(1)$ geometrical factor. For bath temperatures above λJ, the diffusivity will generically saturate to a temperature-independent value, $D_B \propto \lambda J/\hbar$ [35], implying that $t_{\rm eq} \sim L_S^2(\lambda J/\hbar)^{-1}$.

To verify these dynamics, we simulate the evolution of a finite-energy density pure state using the TEBD-algorithm [36]. It is exponentially difficult to simulate finite temperature dynamics and our simulations require an MPS bond-dimension of $m = 20,000$, limiting our system to $L = 30$ sites (Fig. 2) [37]. We initialize a uniform state $|\Psi(0)\rangle = e^{-\tau\hat{H}[\lambda_x=1]}|\uparrow\downarrow\uparrow\downarrow\cdots\rangle$, where $\tau = 0.35/J$, resulting in an energy density that corresponds to temperature $T_S = 0.51J$ after local equilibration [38]. The system is then quenched into a spatially non-uniform $\hat{H}[\lambda_x]$ (Fig. 2). Using the optimal $\lambda_0 = 0.17$ in the 'bath' leads to a final predicted temperature: $T_{\rm f}^{(q)} = 0.29J$.

The evolution of the local energy density $\langle\lambda_x\hat{h}_x(t)\rangle$ during the cooling quench is depicted in Fig. 2(a). The energy density in region S at time $t = 100/J$ corresponds to $T_S = 0.34J$, within 14% of the expected $T_{\rm f}^{(q)}$ [33]. Moreover, the relaxation dynamics are roughly consistent with $T_S \sim T_{\rm f}^{(q)} + (T_{\rm i} - T_{\rm f}^{(q)})\sqrt{t_{\rm eq}/t}$, where $t_{\rm eq} \approx 0.22(\mathcal{K}L_S)^2(\lambda J/\hbar)^{-1}$, consistent with the expectation $1/D_B \sim 0.19/\lambda$ [33, 35].

Even for a relatively small bath size, the cooling quench has a dramatic effect on the dynamical correlation function of the topological edge mode. Since the edge state in region S will generically have overlap with the right-most spin $S^{\mu}_{\rm end}$, its coherence can be probed via the correlation function

$$C_{zz}(t) = \langle\Psi|\, S^z_{\rm end}(t+t_f)S^z_{\rm end}(t_f)\,|\Psi\rangle\,, \qquad (5)$$

where the measurement only begins after the cooling quench is complete ($t_f = 100/J$). At $T = 0$, these correlations should asymptote to a finite constant [Fig. 3a], while at large T [Fig. 3d], they will decay exponentially. We compare $C_{zz}(t)$ under four preparation scenarios described in Fig. 3. The conformal cooling quench improves the coherence time by more than an order of magnitude.

Adiabatic conformal cooling in the fermionic Hubbard model—We next consider the adiabatic protocol applied to the fermionic Hubbard model, $H = -\sum_{<i,j>,\sigma} t_{ij}c^{\dagger}_{i\sigma}c_{j\sigma} + U\sum_i n_{i\uparrow}n_{i\downarrow} - \mu\sum_{i\sigma} n_{i\sigma}$. Here, we focus on the Mott insulating phase at half-filling with $t/U \ll 1$ and $T < U$. While the fermions' motion is quenched, their spins interact via an effective anti-ferromagnetic Heisenberg interaction, $H_{\rm eff} = \sum_{\langle i,j\rangle} J_{ij}[\mathbf{S}_i \cdot \mathbf{S}_j - \frac{1}{4}]$, where $J = 4\frac{t_{ij}^2}{U}$ is the super-exchange coupling.

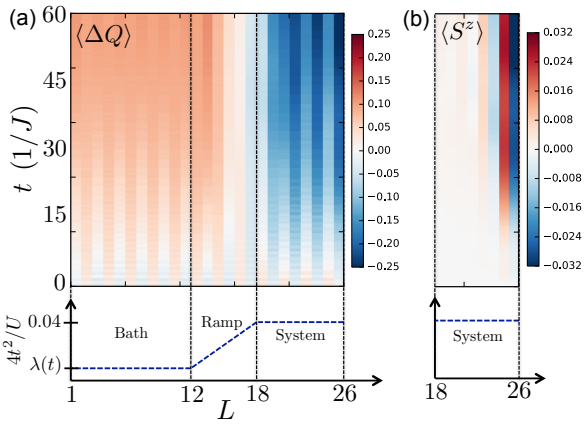

FIG. 5. Cooling dynamics in the 1D spinful Hubbard model. a) After initializing a $T = 1.4J$ thermal state with uniform Hamiltonian $U = 1, t_{ij} = 0.1$, the hopping t_{ij} is adiabatically decreased with a spatial profile shown in the bottom panel. b) Depicts the onset of antiferromagnetic correlations. The right-most site has a small Zeeman field $0.05S^z$. While the initial temperature disorders the spins, as the system cools, algebraic anti-ferromagnetic correlations clearly emerge.

In the Mott regime, adiabatic cooling is naturally realized if one can weakly modulate the depth of the optical potential, $V(\vec{x}) = -V_0(\vec{x}) \sum_{i=1}^{d} \cos(k\, x^i)^2$, where $V_0(\vec{x})$ is slowly varying. Changing V_0 has three effects on the effective Hamiltonian: U will increase, as the orbitals are further localized, μ will increase, as the trap is deeper and t will decrease due to the barrier height. Since t is exponentially more sensitive than U to the trap-depth, $\xi = \sqrt{\frac{V_0}{E_r}}$ (E_r is the recoil energy), the dominant effect is to modulate the hoppings [39]. Assuming μ is compensated to maintain half-filling, the super-exchange energy becomes $J_{ij} \propto \xi^2(x) e^{-4\xi(x)}$, precisely the desired modulation (Fig. 4b). Fortuitously, a small modulation in V_0 is already capable of dramatically reducing the system's temperature; for example, in the the 3D cubic Heisenberg model, a 6% change in the trap depth can cool the system from $1.4T_{\rm N}$ [40] down to the Néel temperature, $T_{\rm N}$ [33]. While the above discussion assumed that $t/U \ll 0, T \ll U$, using determinantal Quantum Monte Carlo, we find that cooling occurs even *outside* the Mott regime, so long as the initial entropy is less than $k_B \log(2)$ [33].

To confirm the effectiveness of the adiabatic protocol, we simulate the dynamics of the spinful 1D fermionic Hubbard model. We use a purified TEBD method to time evolve a finite-temperature ensemble [41]. At time $t = 0$ the Hamiltonian is uniform, $U = 1, t_{ij} = 0.1$, with an initial thermal state $\rho = e^{-H/T_{\rm i}}/\mathcal{Z}$ at $T_{\rm i} = 1.4J$. We then time evolve the ensemble with a Hamiltonian in which t_{ij} decreases adiabatically in the bath. Since energy is not conserved, we divide it into heat and work, $\dot{E} = \dot{Q} - \dot{W}$ [33], and plot the evolution of the heat-density Q in Fig. 5(a). Total heat is conserved, but with clear transport from S to B. As a more qualitative thermometer, we note that at $T = 0$, the system should display algebraic anti-ferromagnetic correlations. To reveal them, we place a small Zeeman field $H = 0.05S^z$ on the right edge spin, both in the initial thermal state and the subsequent dynamics. As depicted in Fig. 5, the finite temperature of the initial thermal state disorders the magnetization $\langle S^z \rangle$, but as the dynamics proceed and cooling occurs, the antiferromagnetic correlations become clearly manifest.

Experimental implementation—Our conformal cooling protocols are well suited to systems with long-ranged interactions, such as polar molecules, Rydberg atoms, and trapped ions [24, 44–47]. To implement the quench protocol, we envision a setup where the average spacing between particles is larger in the bath than in the system, $r_B > r_S$. Assuming power-law interactions ($1/R^\alpha$), the Hamiltonian in B will be reduced by a constant factor $\lambda = (r_S/r_B)^\alpha$ relative to that in S (Fig. 1b). This approach is particularly applicable to current polar molecule experiments where the optical lattice filling, $\nu < 1$, leads to random dilution [24]. Fortunately, the cooling quench is perhaps *simplest* to implement in this randomly diluted case, since one can make $r_B > r_S$ merely by modulating the average density, without having to ensure the particles in B lie on a particular sub-lattice. In this case, simply time-evolving an initial product state in the presence of this density modulation will cool the high-density region, and could provide a simple route towards studying, for example, algebraically correlated random-singlet phases [48–50].

We now propose an experimental route toward realizing the adiabatic cooling protocol in a cold-atomic fermi-Hubbard simulation [17–19]. The key challenge is the generation of a modulated optical potential, $V_0(\vec{x})$, while keeping the chemical potential nearly constant. While the required change in trap depth is modest, the modulated potential nonetheless requires the ability to create two differing lattice potentials in the system and bath regions. The intermediate transitional region does not need to be spatially sharp and a "ramp" region (Fig. 5) will help to ensure that thermal diffusion remains efficient across this boundary.

In principle, a quantum gas microscope combined with digital mirror devices or spatial light modulators allows one to paint a near-arbitrary optical potential. However, since we require only the special case of a "binary" optical potential, we propose a simpler strategy based upon overlaying two distinct optical intensity patterns that are projected onto a single object plane. Rather than using a mirror for retro-reflection, each of the lattices B, S can be generated by two incoming counter-propogating beams, for a total of four beams: B_1, B_2, S_1, S_2 (Fig. 4a). By modulating the intensity of both B_1 and B_2, one can independently control the periodic component V_0 and the slow component μ (likewise for S). Before reaching the object plane, we envision a binary spatial filter that transmits pattern S_1, S_2 to the system's spatial region and pattern B_1, B_2 to the bath's spatial region. Such spatial filtering can be easily achieved in two ways: 1) by utilizing a spatially patterned wave-plate followed by a polarizing filter or 2) by using a dichroic interference filter (Fig. 4a).

In summary, we have proposed a general method for prepar-

ing low-entropy many-body states in isolated quantum systems. Our approach can be naturally implemented in systems with power law interactions by simply diluting the particle density of the bath region; moreover, we also provide a simple experimental blueprint for implementing conformal cooling in the spinful fermionic Hubbard model. Looking forward, our proposal raises a number of intriguing questions: is it possible to implement a refrigeration cycle by repeated preparation of the bath state? Can one optimize a side-by-side geometry which could reduce the equilibration time? By performing conformal cooling during a quantum phase transition, can one reduce the rate of defect formation?

We thank Randy Hulet, Chris Laumann, David Weld, Jun Ye, and Martin Zwierlein for insightful suggestions and illuminating conversations. We acknowledge the QUEST-DQMC collaboration [51] for providing the code used in our QMC calculations. This work was supported in part by the AFOSR through the MURI program, the NSF, the President's Research Catalyst Award CA-15-327861 from the University of California Office of the President, and the Miller Institute for Basic Research in Science. This research was completed at the Kavli Institute for Theoretical Physics, which is supported in part by the National Science Foundation under Grant No. NSF PHY-1125915

[1] A. Leanhardt, T. Pasquini, M. Saba, A. Schirotzek, Y. Shin, D. Kielpinski, D. Pritchard, and W. Ketterle, Science **301**, 1513 (2003).
[2] T. Kovachy, J. M. Hogan, A. Sugarbaker, S. M. Dickerson, C. A. Donnelly, C. Overstreet, and M. A. Kasevich, Phys. Rev. Lett. **114**, 143004 (2015).
[3] M. Anderson, J. Ensher, M. Matthews, C. Wieman, and E. Cornell, science **269**, 14 (1995).
[4] K. B. Davis, M.-O. Mewes, M. R. Andrews, N. Van Druten, D. Durfee, D. Kurn, and W. Ketterle, Phys. Rev. Lett. **75**, 3969 (1995).
[5] B. DeMarco and D. S. Jin, Science **285**, 1703 (1999).
[6] C. Chin, M. Bartenstein, A. Altmeyer, S. Riedl, S. Jochim, J. H. Denschlag, and R. Grimm, Science **305**, 1128 (2004).
[7] M. Schreiber, S. S. Hodgman, P. Bordia, H. P. Lüschen, M. H. Fischer, R. Vosk, E. Altman, U. Schneider, and I. Bloch, Science **349**, 842 (2015).
[8] A. M. Kaufman, B. J. Lester, and C. A. Regal, Physical Review X **2**, 041014 (2012).
[9] A. Kaufman, B. Lester, C. Reynolds, M. Wall, M. Foss-Feig, K. Hazzard, A. Rey, and C. Regal, Science **345**, 306 (2014).
[10] R. Olf, F. Fang, G. E. Marti, A. MacRae, and D. M. Stamper-Kurn, Nature Physics **11**, 720 (2015).
[11] D. M. Stamper-Kurn, Physics **2**, 80 (2009).
[12] G. Campbell, Nature **480**, 463 (2011).
[13] N. Y. Yao, A. V. Gorshkov, C. R. Laumann, A. M. Läuchli, J. Ye, and M. D. Lukin, Phys. Rev. Lett. **110**, 185302 (2013).
[14] Quantum Monte Carlo estimates for the entropy density required for magnetic ordering are: $\sim 0.03k_B$ and $\sim 0.3k_B$ for bosons in two- and three-dimensional lattices, respectively, with similar values for the Neel ordering of fermions. On the experimental front, spin gradient demagnetization of bosons has reached $\sim 0.05k_B$ [52], while evaporative cooling has reached $\sim 10^{-3}k_B$ [10]. For Fermions, $\sim 0.06k_B$ has been reached unitary Fermi gases [53], while $\sim 0.76k_B$ has been achieved in a 3D optical lattice [17]. Antiferromagnetic correlations have also been observed in a 2D Fermi-Hubbard model using quantum gas microscopy [18, 19].
[15] C.-L. Hung, X. Zhang, N. Gemelke, and C. Chin, Phys. Rev. Lett. **104**, 160403 (2010).
[16] S. Chu, Nature **416**, 206 (2002).
[17] R. A. Hart, P. M. Duarte, T.-L. Yang, X. Liu, T. Paiva, E. Khatami, R. T. Scalettar, N. Trivedi, D. A. Huse, and R. G. Hulet, Nature **519**, 211 (2015).
[18] M. F. Parsons, A. Mazurenko, C. S. Chiu, G. Ji, D. Greif, and M. Greiner, arXiv preprint arXiv:1605.02704 (2016).
[19] L. W. Cheuk, M. A. Nichols, K. R. Lawrence, M. Okan, H. Zhang, E. Khatami, N. Trivedi, T. Paiva, M. Rigol, and M. W. Zwierlein, arXiv preprint arXiv:1606.04089 (2016).
[20] A. S. Sørensen, E. Altman, M. Gullans, J. Porto, M. D. Lukin, and E. Demler, Physical Review A **81**, 061603 (2010).
[21] M. Barkeshli, N. Yao, and C. Laumann, Phys. Rev. Lett. **115**, 026802 (2015).
[22] J. Catani, G. Barontini, G. Lamporesi, F. Rabatti, G. Thalhammer, F. Minardi, S. Stringari, and M. Inguscio, Phys. Rev. Lett. **103**, 140401 (2009).
[23] D. Greif, G. Jotzu, M. Messer, R. Desbuquois, and T. Esslinger, Phys. Rev. Lett. **115**, 260401 (2015).
[24] S. A. Moses, J. P. Covey, M. T. Miecnikowski, B. Yan, B. Gadway, J. Ye, and D. S. Jin, Science **350**, 659 (2015).
[25] A familiar example of such an approach is magnetic refrigeration, for which $H \sim \mathbf{B}(t) \cdot \mathbf{m}$, where $\mathbf{B}$ is an external magnetic field and $\mathbf{m}$ the magnetization [54, 55].
[26] S. Braun, J. P. Ronzheimer, M. Schreiber, S. S. Hodgman, T. Rom, I. Bloch, and U. Schneider, Science **339**, 52 (2013).
[27] T. Müller, S. Fölling, A. Widera, and I. Bloch, Phys. Rev. Lett. **99**, 200405 (2007).
[28] G. Wirth, M. Ölschläger, and A. Hemmerich, Nature Physics **7**, 147 (2011).
[29] In 1D and 2D, it may be possible to place S and B "side-by-side," so that their contact scales extensively with their volume. This arrangement could reduce the equilibration time, since one no longer requires diffusion. However, the coupling between S and B now has a non-trivial contribution to the thermodynamics and it's effect would have to be accounted for in detail.
[30] F. D. M. Haldane, Phys. Rev. Lett. **50**, 1153 (1983).
[31] I. Affleck, T. Kennedy, E. H. Lieb, and H. Tasaki, Phys. Rev. Lett. **59**, 799 (1987).
[32] C. Senko, P. Richerme, J. Smith, A. Lee, I. Cohen, A. Retzker, and C. Monroe, Phys. Rev. X **5**, 021026 (2015).
[33] See supplementary information.
[34] K. Damle and S. Sachdev, Phys. Rev. B **57**, 8307 (1998).
[35] J. Karadamoglou and X. Zotos, Phys. Rev. Lett. **93**, 177203 (2004).
[36] G. Vidal, Phys. Rev. Lett. **91**, 147902 (2003).
[37] We work at $\gamma = \frac{3}{4}$, which reduces the correlation length relative to $\gamma = 0$ but is otherwise completely generic.
[38] Note that while this state seems contrived from an experimental perspective, it is convenient to prepare numerically, and owing to ergodicity the only relevant characteristic is its energy density.
[39] W. Hofstetter, J. I. Cirac, P. Zoller, E. Demler, and M. Lukin, Phys. Rev. Lett. **89**, 220407 (2002).
[40] R. A. Hart, P. M. Duarte, T.-L. Yang, X. Liu, T. Paiva, E. Khatami, R. T. Scalettar, N. Trivedi, D. A. Huse, and R. G. Hulet, Nature (London) **519**, 211 (2015), arXiv:1407.5932.

[41] C. Karrasch, J. H. Bardarson, and J. E. Moore, New Journal of Physics **15**, 083031 (2013).
[42] A.-M. Daré, L. Raymond, G. Albinet, and A.-M. S. Tremblay, Phys. Rev. B **76**, 064402 (2007).
[43] T. Paiva, R. Scalettar, M. Randeria, and N. Trivedi, Phys. Rev. Lett. **104**, 066406 (2010).
[44] B. Yan, S. A. Moses, B. Gadway, J. P. Covey, K. R. Hazzard, A. M. Rey, D. S. Jin, and J. Ye, Nature **501**, 521 (2013).
[45] J. Zeiher, R. van Bijnen, P. Schauß, S. Hild, J.-y. Choi, T. Pohl, I. Bloch, and C. Gross, arXiv preprint arXiv:1602.06313 (2016).
[46] J. Smith, A. Lee, P. Richerme, B. Neyenhuis, P. W. Hess, P. Hauke, M. Heyl, D. A. Huse, and C. Monroe, arXiv preprint arXiv:1508.07026 (2015).
[47] E. A. Martinez, C. Muschik, P. Schindler, D. Nigg, A. Erhard, M. Heyl, P. Hauke, M. Dalmonte, T. Monz, P. Zoller, *et al.*, arXiv preprint arXiv:1605.04570 (2016).
[48] A. V. Gorshkov, S. R. Manmana, G. Chen, J. Ye, E. Demler, M. D. Lukin, and A. M. Rey, Phys. Rev. Lett. **107**, 115301 (2011).
[49] N. Y. Yao, M. P. Zaletel, D. M. Stamper-Kurn, and A. Vishwanath, arXiv preprint arXiv:1510.06403 (2015).
[50] D. S. Fisher, Physical Review B **50**, 3799 (1994).
[51] R. L. Sugar, D. J. Scalapino, S. R. White, E. Y. Loh, and R. Scalettar, "Quantum electron simulation toolbox," .
[52] P. Medley, D. M. Weld, H. Miyake, D. E. Pritchard, and W. Ketterle, Phys. Rev. Lett. **106**, 195301 (2011).
[53] M. J. Ku, A. T. Sommer, L. W. Cheuk, and M. W. Zwierlein, Science **335**, 563 (2012).
[54] P. Debye, Annalen der Physik **386**, 1154 (1926).
[55] W. F. Giauque, Journal of the American Chemical Society **49**, 1864 (1927), http://dx.doi.org/10.1021/ja01407a003.

Thermodynamics of the quench protocol for the $S = 1$ chain

Here we report the final system energy density, entropy density, and temperature as a function of both the initial energy density in units of the gap, E_i/Δ, and the ratio of bath to system length L_B/L_S. The thermodynamic relation $T(E)$ was computed using exact diagonalization Eq. (3) for 10-site chain, which we then use to numerically solve Eq. (1). A table of results is reported in Fig. 6.

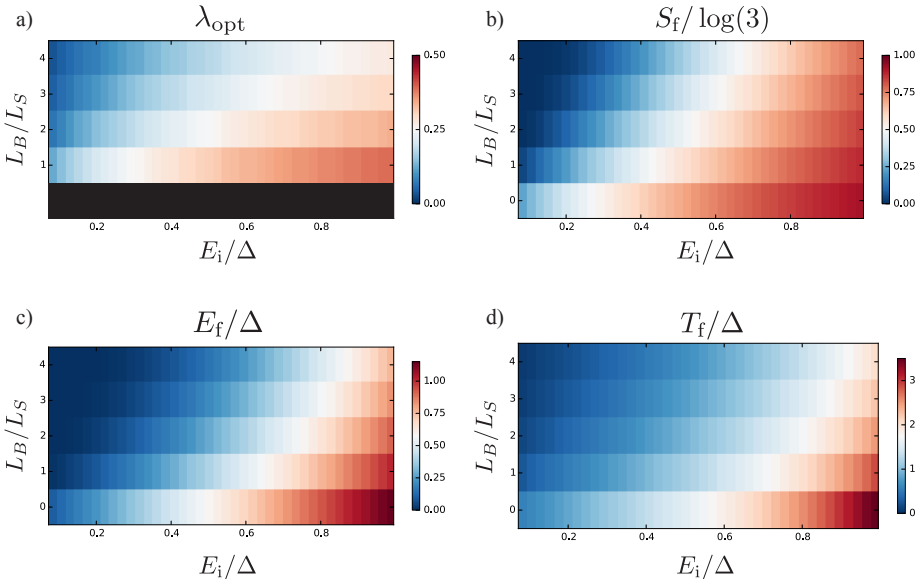

FIG. 6. Thermodynamics of the cooling quench for a spin-1 Heisenberg chain at $\gamma = 3/4$ (results for other γ are similar). The final state of the system depends on the ratio of bath to system size, L_B/L_S, and the initial energy density above the ground state in unit of the gap, E_i/Δ. For comparison, the state $|\uparrow\downarrow\cdots\rangle$ is at $E_\mathrm{i}/\Delta = 0.54$. (**a**) The optimal choice of bath scaling λ_opt. Larger baths allow for smaller λ_opt, and hence greater cooling. (**b**) The final system entropy S_f in units of the infinite-temperature value $\log(3)k_B$. (**c**) The final system energy density above the ground state, E_f, in units of the gap. (**d**) The final system temperature, T_f, in units of the gap.

Diffusion times for the cooling quench

Solving the heat diffusion equation exactly is not possible, since the temperature dependence of the heat capacity and thermal conductivity leads to a non-linear PDE that depends on the details of the model. As an illustrative approximation, note that temperature gradients in S decay exponentially over the diffusion time $t_S \sim L_S^2/D_S$, while when V_B is large the average

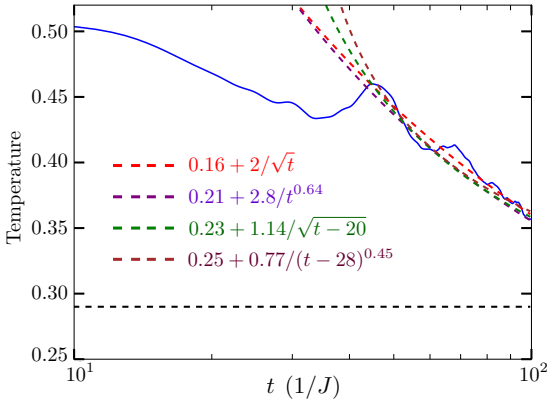

FIG. 7. The system temperature $T_S(t)$ at time t of the Haldane-chain cooling quench shown in Fig. 2 of the main text. T_S is inferred by measuring the energy density at the center of S, using the thermodynamic relation $T_S(E)$ computed from exact diagonalization. Unfortunately we can only evolve out to about $t = 100/J$ (which takes several weeks of computing time), so it is difficult to tell how well the decay matches the expected $\sqrt{t_{\rm eq}/t}$ behavior. The predicted final temperature is shown as a horizontal dashed line, though a deviation due to finite size effects would be expected for such a small system. Various ansatz fits our shown, which show rough consistency with the expected $1/\sqrt{t}$ behaviour.

temperature T_S of the system decays as a much slower power law, $T_S \sim 1/\sqrt{t}$. Since the dynamics of T_S are so much slower than the dynamics of the temperature gradients in S, we can consider a simplified model which lumps the system together into a single heat capacity $C_S(T_S) = V_S c_S(T_S)$. As for the bath, we assume it is at a relatively high temperature in terms of the natural units λJ. In a high-temperature expansion for a spin model, both the heat capacity and thermal conductance scale as $1/T^2$, so the diffusivity $D_B = \kappa/c$ is nearly constant ($D_B = 5.3\lambda J/\hbar$ for the AKLT chain [35]). Thus we consider a continuous medium of diffusivity D_B coupled to a single heat capacity C_S, where at time $t = 0$ the system temperature is $T_S = T_i$ and the bath temperature is $T_B = \lambda T_i$. Ignoring the temperature dependence of c_S/c_B, Fourier's law can be solved to obtain

$$T_S(t) \sim T_{\rm f} + \mathcal{K}\frac{c_S}{c_B}\frac{L_S}{\sqrt{tD_B}}(T_{\rm i} - T_{\rm f}). \tag{6}$$

where $\mathcal{K}$ is an order-one geometrical factor and $T_{\rm f}$ is the final equilibrium temperature. After the system reaches $T_S < \Delta$, with Δ the gap, c_S/c_B will decrease exponentially with T_S (since the system's heat capacity is activated), so ignoring the temperature dependence of c_S/c_B is no longer justified. This does not accelerate the cooling, however; the $t^{-1/2}$ behavior will remain since the temperature gradient in the *bath* must still relax. In Fig. 7, we show $T_S(t)$ for the cooling quench of the Haldane model.

Definition of Q for adiabatic quench.

In the adiabatic protocol the Hamiltonian $H(t) = \sum_i h_i(t)$ changes in time, so energy is not conserved. Nevertheless, we would like a convenient way to show heat is being transported between the bath and system. For a large system we could use the local temperature as inferred from the local energy density, but for the small chains studied here we find artifacts near the edge and ramp which make it less useful to visualize.

Instead, we note that the energy changes according to $\partial_t E = \sum_i \langle t| (\partial_t h_i) |t\rangle$, and that the change in energy can be divided into the heat Q and work W, $dE = \delta Q - \delta W$. In the adiabatic limit $\delta Q = 0$ globally, but heat can be transported between regions (of course transport of energy is driven by entropy production, so this transport itself must be arbitrarily slow in the adiabatic limit). This motivates the definition $Q = \sum_i Q_i$ where $\partial_t Q_i = \partial_t(\langle t| h_i |t\rangle) - \langle t| (\partial_t h_i) |t\rangle$. By construction $\partial_t Q = 0$, though each Q_i may change. It is these Q_i which are shown in the Fig. 5 of the main text. The practical implementation of this subtraction is illustrated in Fig.8.

While the Q_i can be defined in this manner away from the adiabatic limit, and $\sum_i Q_i$ is always constant, it does not have the precise definition of 'heat,' since the diffusive transport itself generates entropy, and hence heat TdS. Note, however, that in the system $\partial_t h_i = 0$, so there Q_i reduces to the energy density. Since our experiment shows $\partial_t Q_i < 0$ in the system, it is unambiguously cooling.

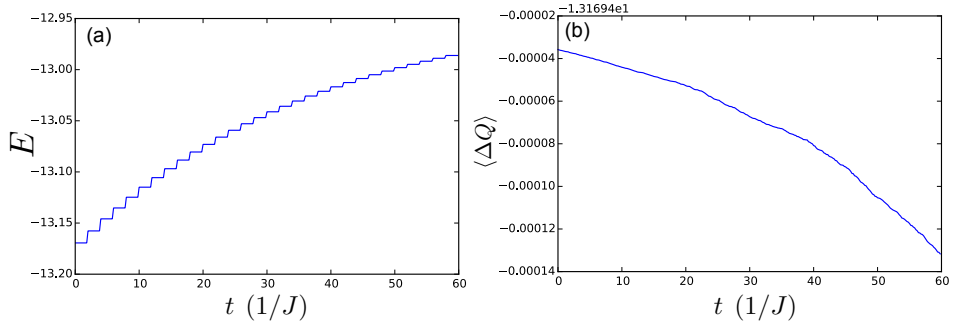

FIG. 8. (a) Total energy E as a function of time for the 1D Hubbard simulations. For numerical convenience, the coupling constants are changed in a series of small, discrete steps, leading to step-discontinuities in the energy interlaced with periods of E-conserving evolution. Likewise, the local energy density E_i has step-discontinuities interlaced with slow dynamics. Q_i is conveniently obtained from the E_i by dropping all the step-discontinuities. (b) The total Q is conserved to better than $10^{-4}J$; the error aries from numerical errors like the finite Trotter step used in the finite-temperature TEBD dynamics.

Adiabatic cooling of Hubbard model outside the Mott regime

The analysis of the Hubbard model in the main text assumed the Mott limit $t/U \to 0$, so that t, U only appear through the super-exchange energy $J = 4\frac{t^2}{U}$. To confirm the approach is effective outside the Mott regime, we note that for the adiabatic cooling to work we only require that the temperature satisfies $\partial_t T(s; t, U) > 0$, where s is the entropy density. Using determinantal quantum Monte Carlo to determine T for the 2D Hubbard model, we see this condition it satisfied whenever $s < \log(2)k_B$.[42]

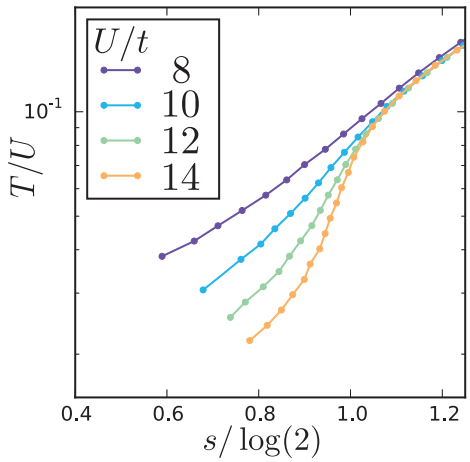

FIG. 9. Thermodynamics of the 2D fermionic Hubbard model: dependence of the temperature T on the entropy density s and the model parameters t, U, at half-filling. We see that at fixed entropy, $\partial_t T|_s > 0$ whenever $s < \log(2)k_B$, implying the adiabatic scheme works outside the Mott limit. Calculations were done using the QUEST DQMC package on an 8×8 torus with extrapolation of the Trotter step to zero.